Results in Engineering 32 (2026) 111694

Contents lists available at ScienceDirect

Results in Engineering

journal homepage: www.sciencedirect.com/journal/results-in-engineering

Research paper

Experimental characterization and luminance simulation of light propagation in smoke-filled environments

J. Quintana Benito [a,*], B. Garcia-Fernandez [b], A. Álvarez Fernández-Balbuena [c], M. Duvisón Rodriguez [c], M. Jaureguizar Ortiz [d], M. A. Garcia Perez [d], D. Váquez Molini [c]

[a] Universidad Europea de Madrid, Calle Tajo, Villaviciosa de Odón, Madrid, 28670,
[b] Universidad Politécnica de Madrid, José Antonio Novais, 10, Madrid, Madrid, 28040,
[c] Universidad Complutense de Madrid, Calle Arcos de Jalón, Madrid, Madrid, 28037,
[d] Normagrup, Parque Tecnológico de Asturias, Parcela 10, Asturias, 33424,

ARTICLE INFO

Keywords:
Fire
Smoke visibility scene
Smoke and light scattering
Smoke chamber
Smart lighting
Simulated smoke scene

ABSTRACT

Smoke generated during a fire modifies light propagation through absorption and scattering processes caused by suspended particles, reducing visibility in indoor environments. The optical characterization of these aerosols is relevant for analyzing how different smoke conditions affect light distribution and visual perception in spaces equipped with emergency lighting systems.

This work presents an experimental methodology to study the interaction between light and smoke under controlled laboratory conditions. First, the spectral extinction coefficient is experimentally determined for different combustion materials through light transmittance measurements. Subsequently, the angular distribution of scattered light is analyzed.

The experimentally obtained optical parameters are then incorporated into a lighting simulation tool intended for analyzing the spatial luminance distribution in scenarios with defined optical properties. The results reveal differences in the spectral and angular behavior of smoke generated by different materials, highlighting the influence of aerosol properties on light propagation.

This study is limited to the experimental conditions considered and does not aim to establish a universal model for the optical behavior of fire smoke. Nevertheless, the proposed methodology provides a useful framework for combining experimental optical characterization and lighting simulation in smoke-filled environments.

1. Introduction

Smoke generated during a fire is one of the main factors limiting visibility and the ability of occupants to orient themselves during evacuation. From an optical perspective, smoke can be described as an aerosol composed of gases and suspended particles. In smoke-filled environments, the light reaching an observer or a surface is attenuated due to absorption and scattering processes caused by suspended combustion particles. Therefore, the effectiveness of emergency lighting systems in smoke-filled environments depends not only on the emitted luminous intensity, but also on the interaction between radiation and suspended particles, as well as on the observer position [1–9].

To evaluate visibility loss in these environments, it is necessary to characterize the behavior of light when interacting with the aerosol. In this context, the extinction coefficient quantifies the attenuation of radiation along an optical path, while the phase function describes the angular distribution of scattered light. Both parameters depend on the physical properties of the smoke, including particle concentration, particle size distribution, fuel type, and combustion conditions [10–15].

Several studies have analyzed the optical behavior of aerosols generated from the combustion of different materials, establishing relationships between particle size distribution, extinction coefficient, and the spectral dependence of light propagation [16–19]. These studies show the variability of smoke optical properties depending on the combustible material and demonstrate the visibility loss associated with smoke-filled environments [20,21]. In addition, many of these studies focus exclusively on transmittance or visibility measurements, without simultaneously considering the angular distribution of scattered light and its influence on the luminance perceived by an observer. Furthermore, the experimental characterization of spectral attenuation and angular

* Corresponding author.
E-mail address: jaime.quintana@universidadeuropea.es (J. Quintana Benito).

https://doi.org/10.1016/j.rineng.2026.111694
Received 18 March 2026; Received in revised form 3 June 2026; Accepted 22 June 2026
Available online 26 June 2026

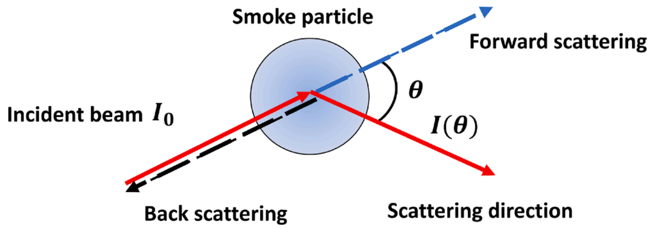

Fig. 1. Phase function diagram.

scattering is not always subsequently incorporated into lighting simulation tools capable of reproducing the spatial luminance distribution in scenarios with defined optical properties.

The aim of this work is to study the interaction between light and smoke through the experimental determination of the spectral extinction coefficient and the analysis of angular scattering distribution for different materials and, subsequently, to integrate these results into a simulation tool for analyzing the luminance perceived by an observer. To this end, an experimental methodology is presented to characterize spectral extinction and angular light scattering in smoke-filled environments under controlled laboratory conditions. The obtained optical parameters are subsequently incorporated into a luminance simulation model in order to analyze light distribution trends in smoke-affected environments.

2. Optical principles of smoke-light interaction

Aerosols are media containing suspended particles that scatter light in multiple directions. This scattering phenomenon is related to the size and geometry of the particles forming the smoke. Mie theory describes the scattering of electromagnetic waves by spherical particles when the incident wavelength is comparable to the size of the scattering particles. Based on this theory, optical parameters such as the phase function can be obtained, representing the angular distribution of radiation scattered by the aerosol [1,16,19,22–25].

$$P(\theta) = \frac{I(\theta)}{I_0}, \tag{1}$$

where $P(\theta)$ represents the relative distribution of scattered intensity at a given angle, $I(\theta)$ is the outgoing intensity at that angle, and I_0 is the incident intensity, as illustrated in Fig. 1. This function is related to the scattering coefficient α_s, allowing the angular redistribution of scattered radiation within the medium to be described [26,27].

On the other hand, when light propagates through an aerosol, the luminous intensity is attenuated as a consequence of absorption by the medium itself. Absorption transforms part of the radiative energy into internal energy of the particles and gases present in the medium. To describe this phenomenon, the absorption coefficient α_a is defined. The combined contribution of both processes is represented by the extinction coefficient [16,28],

$$k_{Ext} = \alpha_s + \alpha_a \tag{2}$$

where α_s represents the scattering coefficient and α_a the absorption coefficient.

In a smoke-filled environment, the attenuation of intensity along a given path can be expressed using the Lambert–Beer law. This relationship allows the transmitted intensity to be related to the incident intensity, the optical path length, and the extinction coefficient of the medium.

$$I = I_0 \cdot e^{-k_{Ext} L} \tag{3}$$

Although this approach presents limitations in highly scattering and non-homogeneous media, the Lambert–Beer law is still commonly used as a first-order approximation for estimating optical extinction trends in combustion aerosols under controlled conditions [17,19,29].

Therefore, the analysis of light–smoke interaction requires simultaneously considering both spectral attenuation and the angular distribution of radiation. In this work, the extinction coefficient is used to evaluate the transmission of different wavelengths through smoke, while angular measurements are employed to analyze how the perceived luminance varies depending on the relative position between the light source, the smoke, and the observer.

The conclusions obtained should be interpreted within the experimental conditions considered, since the optical properties of smoke may vary significantly depending on the combustible material and the aerosol generation conditions.

3. Multispectral approach to characterize the extinction coefficient of smoke

To experimentally characterize the spectral attenuation of light in the presence of smoke, a measurement system based on a transparent methacrylate aerosol chamber was developed, as shown in Fig. 2. The purpose of the system is not to reproduce the complete dynamics of a real fire, but rather to generate controlled and repeatable conditions that allow the optical interaction between radiation and the aerosol generated by different combustion materials to be analyzed.

The experimental system consists of a spectrophotometer, a closed chamber for smoke containment, and a light source, either a continuous-spectrum source or an LED, located close to the spectrophotometer. The emitted light passes through a converging lens that focuses the beam during its propagation through the smoke volume. Subsequently, the radiation is reflected by a mirror and collected by an optical fiber connected to the spectrometer, as shown in the scheme presented in Fig. 3. The mirror forces the beam to traverse the smoke-filled volume twice, providing a well-defined optical path and increasing the effective interaction length between the radiation and the aerosol.

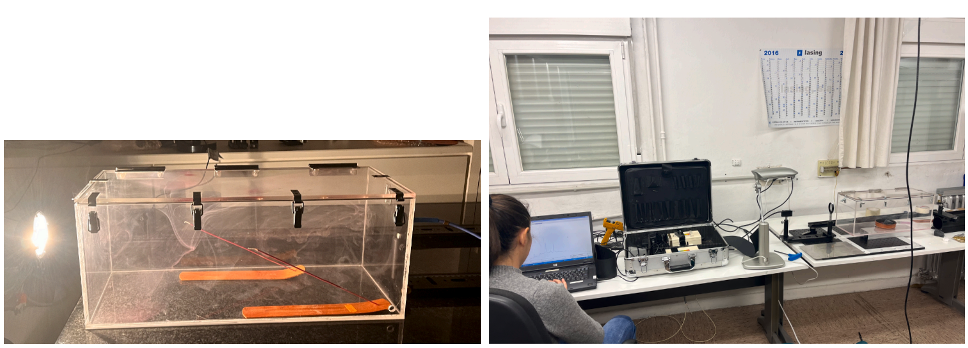

(a) (b)

Fig. 2. (a) Methacrylate chamber employed in the experiments, (b) Multispectral extinction setup.

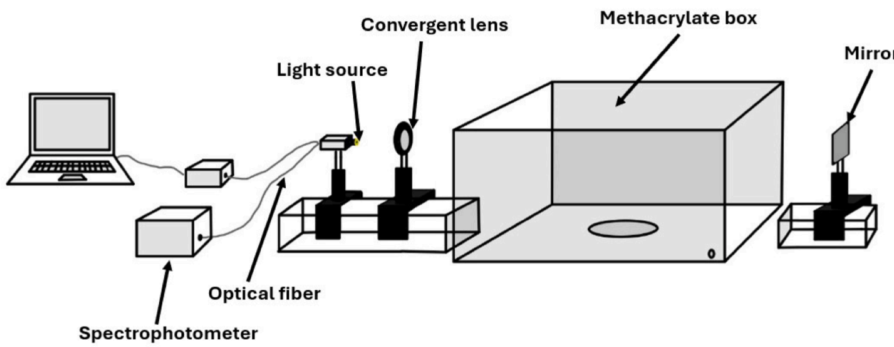

(a)

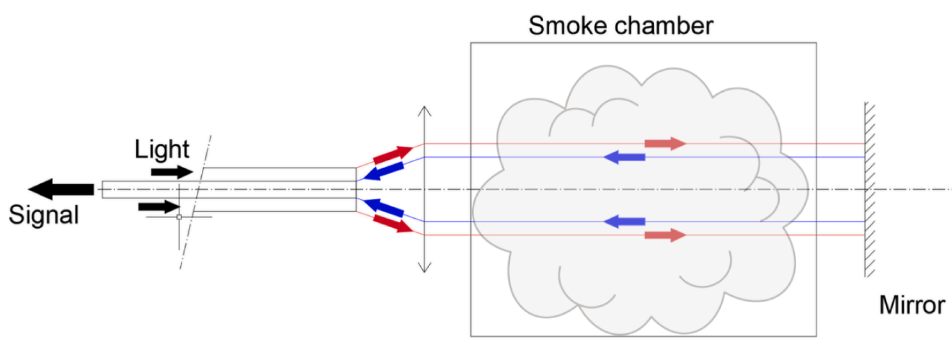

(b)

Fig. 3. (a) Scheme of the setup developed to analyze the multispectral extinction coefficient of light, (b) Representation of light propagation through the chamber and its subsequent detection by the sensor.

The spectrophotometer and the light source are placed at a distance of $20cm$, while the light propagates through a path length of $0.45m$ inside the chamber before reaching the mirror. After reflection, the beam travels back through the same smoke-filled volume and exits the chamber towards the spectrophotometer. Therefore, the total optical path length corresponds to the complete trajectory of the light from its entrance into the chamber to its exit after reflection, yielding ($L = 0.96m$). This configuration allows the transmitted spectral distribution in the presence of smoke to be compared with a reference measurement acquired without aerosol. Based on Eq. (3), the extinction coefficient is determined using this total optical path length.

$$k_{Ext}(\lambda) = \frac{\ln\left(\frac{I_0(\lambda)}{I(\lambda)}\right)}{L} \tag{4}$$

The spectral intensity generated by different combustible materials, including wood, extruded polystyrene, rubber, and incense, was measured, as shown in Fig. 4. The measurement procedure consists of first acquiring a reference measurement in the absence of smoke and subsequently recording measurements at regular time intervals ($15s$) as the combustible material progressively releases smoke. Consequently, the initial measurements correspond to low-smoke conditions, whereas the final measurements represent more opaque scenarios with lower transmitted intensity.

Based on these measurements, the spectral extinction coefficient is calculated using the Lambert–Beer law as a first-order approximation to describe the attenuation of luminous intensity along the optical path. Although this approximation presents limitations in highly scattering and non-homogeneous media, it is useful for estimating relative extinction trends under controlled laboratory conditions, as shown in Fig. 5.

Fig. 4 shows examples of the spectral irradiance distributions obtained for smoke generated by wood and rubber combustion under different illumination conditions. The curves represent the irradiance measured in the presence of aerosol and its comparison with the reference acquired in the absence of smoke. As the opacity of the medium increases, a progressive reduction in transmitted intensity is observed throughout the analyzed spectral range.

Fig. 5 presents the spectral extinction coefficient calculated using the Lambert–Beer law (3). The results show significant differences between the employed light sources, both in the spectral distribution of irradiance and in the spectral dependence of the extinction coefficient. In both cases, attenuation decreases for wavelengths approaching the near-infrared region, indicating a relative increase in transmittance at longer wavelengths. This behavior is consistent with trends previously reported for combustion aerosols generated from other materials [16].

Furthermore, the observed differences between LED illumination and the extended-spectrum source suggest that the spectral distribution of the source significantly influences the radiation–smoke interaction. Measurements performed using LED illumination show a more pronounced spectral dependence, with higher attenuation in the blue region of the visible spectrum and relatively higher transmittance at longer wavelengths. In contrast, the extended-spectrum source exhibits a smoother spectral behavior due to its emission being distributed over a wider wavelength range. In both cases, the interval approximately between 650 and 780 nm exhibits lower relative extinction levels,

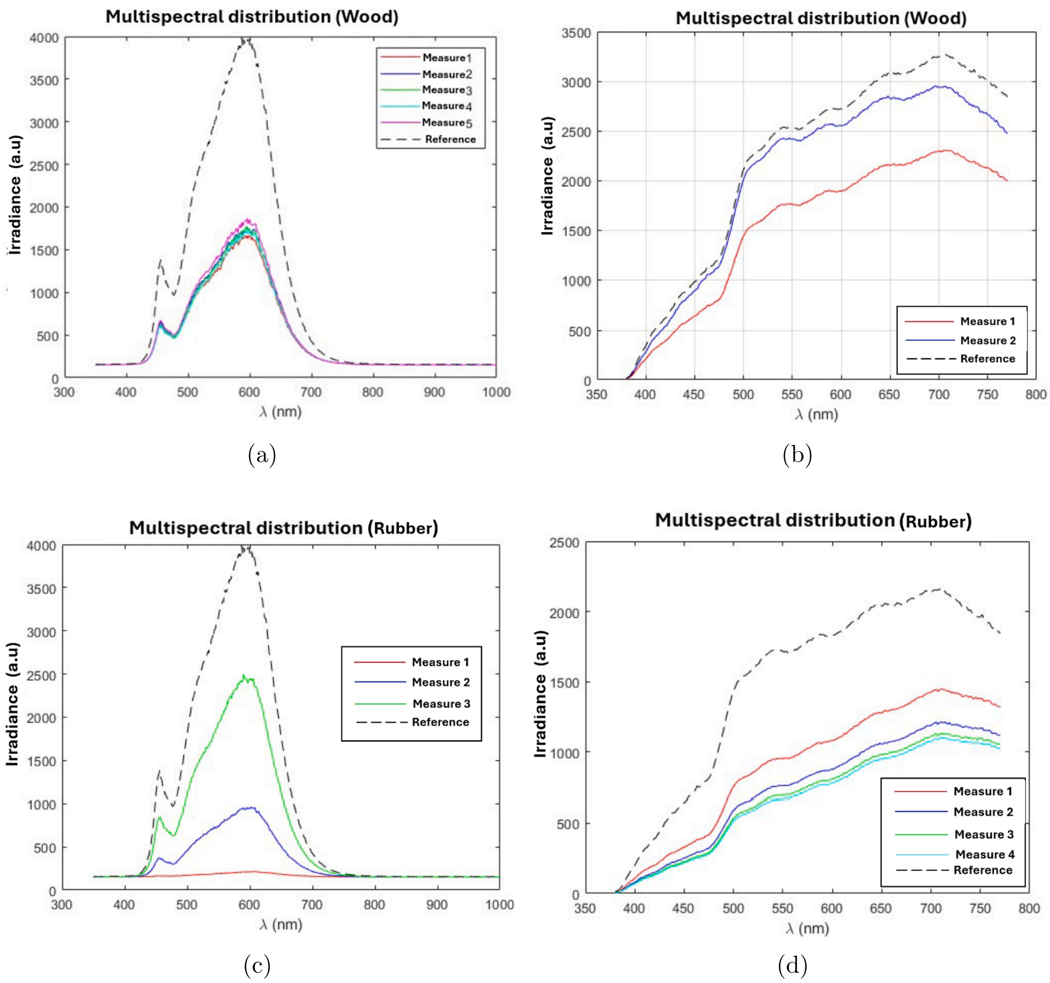

Fig. 4. Experimental measurements of irradiance as a function of wavelength. 4(a) Wood smoke: spectral intensity of an LED source. 4(b) Wood smoke: spectral intensity of a continuous-spectrum source. 4(c) Rubber smoke: spectral intensity of an LED source. 4(d) Rubber smoke: spectral intensity of a continuous-spectrum source.

suggesting that the red to near-infrared region could potentially be favorable for vision and detection applications in smoke-filled atmospheres.

The obtained results indicate that the spectral extinction of radiation depends significantly on the optical properties of the generated aerosol. Certain spectral regions exhibit lower relative attenuation levels, although these trends should not be interpreted as universal, since they are conditioned by the nature of the combustible material and the combustion conditions. In real fire scenarios, particle size distribution, morphology, and concentration may vary considerably, substantially modifying the optical behavior of smoke.

During the experimental tests, soot deposition was observed on the chamber walls and on the optical elements of the measurement system, producing an additional reduction in the signal recorded by the spectrometer. This effect introduces a relevant experimental limitation and suggests that maintaining optical surfaces free of deposits could improve effective visibility in smoke-filled environments.

The absence of a detailed characterization of particle size distribution and morphology limits the direct extrapolation of the results to other combustion scenarios. Nevertheless, the proposed methodology allows the experimental analysis of how different smoke generation conditions modify the spectral transmission of radiation, providing useful optical parameters for future simplified models of light propagation and luminance distribution in aerosol-laden atmospheres. The obtained results also suggest possible future research directions focused on the development and selection of optical systems with improved transmission capability in the presence of smoke. In particular, the design of light sources, sensors, and optical elements optimized for longer wavelengths could contribute to improving the effective transmission of radiation and, consequently, visibility conditions in fire scenarios.

4. Multispectral approach to characterize the angular scattering distribution of smoke

The angular characterization of scattered light was carried out using a sealed smoke chamber measuring 90 × 90 × 220 cm, designed to generate controlled measurement conditions. The experimental system makes it possible to analyze how the luminance perceived by an observer varies depending on the relative direction between the light source, the aerosol, and the detector.

To this end, a luminance meter (Lumincam 1300) was placed at one end of the chamber, while the light source was mounted on a motorized goniometer controlled using Matlab, as shown in Fig. 6. This system allows the illumination angle to be modified and the perceived luminance to be recorded for different geometric configurations. Similarly to the methodology employed for measuring the extinction coefficient, smoke was generated through the combustion of different materials, including wood, extruded polystyrene, rubber, and incense.

The employed luminaire consists of a seven-LED system emitting at different wavelengths: $\lambda = 447.5\ nm$, $\lambda = 470\ nm$, $\lambda = 505\ nm$, $\lambda =$

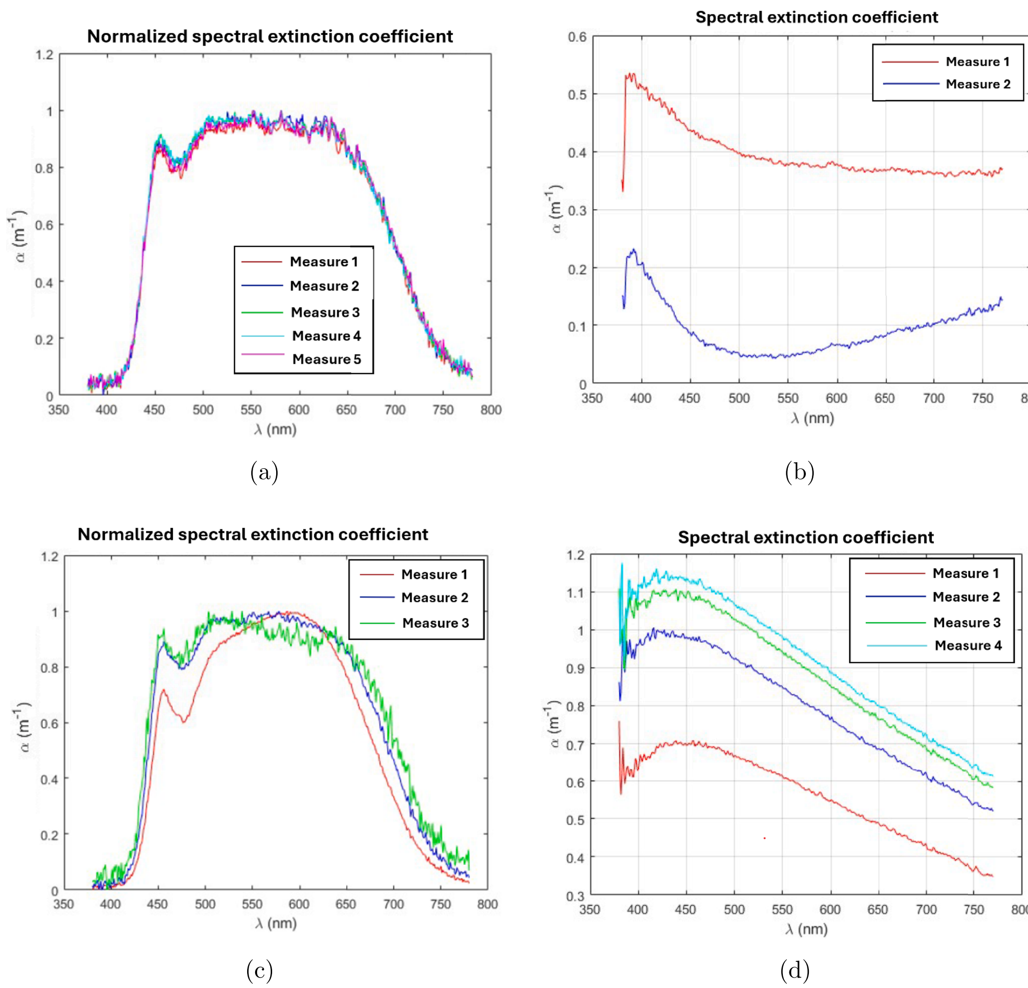

Fig. 5. Spectral extinction coefficient calculated using the Lambert–Beer law from the experimental measurements shown in Fig. 4. 5(a) Wood smoke illuminated with an LED source. 5(b) Wood smoke illuminated with a continuous-spectrum source. 5(c) Rubber smoke illuminated with an LED source. 5(d) Rubber smoke illuminated with a continuous-spectrum source.

530 *nm*, $\lambda = 590$ *nm*, $\lambda = 617$ *nm*, and $\lambda = 627$ *nm*, providing multispectral information about the phase function (1). To avoid interference between the different light sources, converging lenses were placed at the output of each LED in order to focus the beams at different positions.

To ensure the repeatability of the experiment, a series of preliminary measurements was performed over time (2 minutes) to verify the stability of the smoke generated inside the chamber, as shown in Fig. 7.

The measurement procedure consists of the following steps. First, a combustible material is introduced into the chamber and allowed to burn for a few seconds until the chamber volume is filled with smoke. Subsequently, fans located at both ends of the chamber are activated to ensure a uniform smoke distribution throughout the volume. Once a homogeneous distribution is achieved, the optical density of the smoke is determined using the lux meter shown in Fig. 6. The measurement process is then initiated by varying the angular position of the light sources using a goniometer that rotates in increments of 10° up to a maximum angle of 110°, as illustrated in Fig. 8. For each angular position, a measurement is acquired using the Lumicam 1300. Subsequently, all measurements are analyzed using external software (Matlab) in order to relate them to the extinction coefficient of the medium.

The objective of the experimental procedure is not to obtain a complete theoretical description of the angular distribution of radiation scattered by smoke, but rather to experimentally analyze angular scattering trends under controlled conditions. Since aerosol properties depend on both the combustible material and the smoke generation conditions, the obtained results should be interpreted only within the experimental conditions considered in this work (Fig. 9).

The multispectral analysis reveals a dependence of luminance on wavelength. Short wavelengths exhibit larger angular variations and a more pronounced intensity decay, indicating a stronger interaction with smoke particles. In contrast, longer wavelengths maintain relatively more stable values at larger angles, showing lower sensitivity to scattering. This behavior is consistent with the scattering mechanisms predicted by Mie theory for combustion aerosols, particularly the predominance of forward scattering.

On the other hand, smoke generated from incense, wood, rubber, and polyurethane exhibits similar phase functions as the reception angle varies. In contrast, smoke generated from incense shows slight differences at angles close to the principal direction. These differences may be associated with several factors, including combustion type and the characteristics of the generated particles. Incense consists of a mixture of different materials that may produce more complex decomposition products. Consequently, the generated smoke contains additional volatile and aromatic compounds whose optical properties may differ slightly from those of the other analyzed materials.

To provide a more quantitative representation of the angular scattering behavior, Table 1 summarizes representative normalized intensity

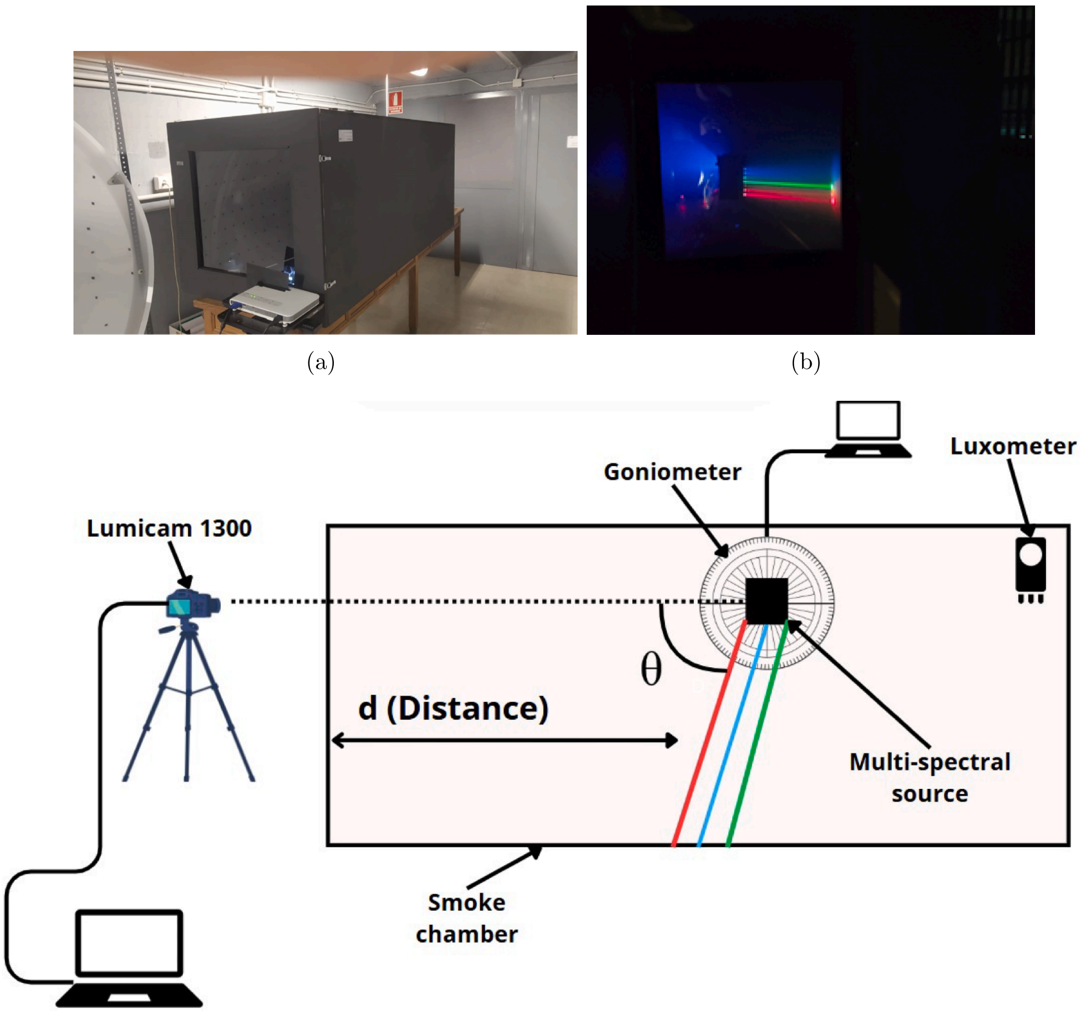

(a) (b) (c)

Fig. 6. Multispectral light propagation inside a smoke chamber. (a) Smoke chamber. (b) Multispectral measurements inside the smoke chamber. (c) Schematic representation of the experimental setup.

Table 1
Normalized scattered intensity distribution for polyurethane smoke as a function of observation angle and wavelength.

Angle (°)	447.5 nm	470 nm	505 nm	530 nm	590 nm	617 nm	627 nm
10	1.000	1.000	1.000	1.000	1.000	1.000	1.000
20	0.716	0.330	0.183	0.228	0.251	0.232	0.311
30	0.327	0.268	0.151	0.112	0.207	0.192	0.261
40	0.150	0.195	0.115	0.073	0.157	0.148	0.201
50	0.069	0.100	0.088	0.050	0.120	0.113	0.155
60	0.022	0.016	0.016	0.032	0.021	0.022	0.034
70	0.014	0.016	0.016	0.023	0.021	0.021	0.034
80	0.021	0.016	0.016	0.014	0.021	0.021	0.033
90	0.021	0.016	0.016	0.010	0.021	0.021	0.033
100	0.021	0.016	0.016	0.009	0.021	0.021	0.033
110	0.021	0.015	0.015	0.008	0.020	0.021	0.032

values obtained for polyurethane smoke under different observation angles and wavelengths. The values were normalized with respect to the intensity measured at the smallest observation angle. The results should be interpreted as relative trends observed under the considered experimental conditions.

The normalized measurements show a progressive decrease in scattered intensity as the observation angle increases. In general, shorter wavelengths exhibit a more pronounced angular attenuation, whereas longer wavelengths maintain relatively higher normalized intensity values at larger angles. This behavior is consistent with the forward-scattering trends expected for combustion aerosols described by Mie scattering theory. Nevertheless, the presented values should not be interpreted as universal phase-function parameters, since they depend on the specific combustion and aerosol generation conditions considered in this work.

5. Simulation tool for evaluating visibility and light scattering in smoke chambers

The experimentally obtained optical parameters were subsequently incorporated into a lighting simulation tool developed to analyze the spatial luminance distribution in environments with defined optical properties. The objective of the simulation is to study relative luminance distribution trends in the presence of smoke using experimentally measured parameters.

The implemented model is not intended to reproduce the complete dynamics of smoke propagation nor to provide a validated prediction of human visual behavior during evacuation. Its purpose is to provide a simplified analysis environment that allows evaluating how certain optical properties of the aerosol affect light propagation and the lumi-

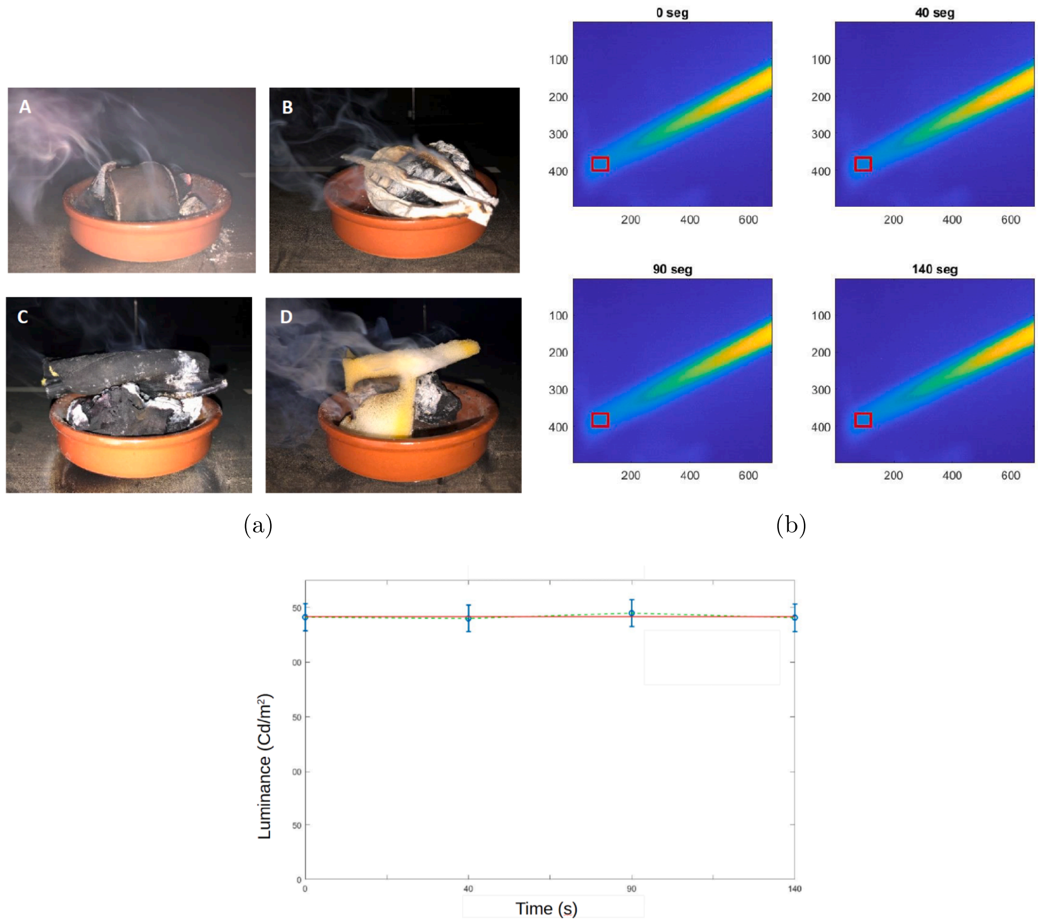

(a) (b)

(c)

Fig. 7. (a) Combustion of different materials (wood, incense, rubber, and polyurethane). (b) Smoke stability measurements acquired using the Lumicam system. (c) Representation of smoke stability over time.

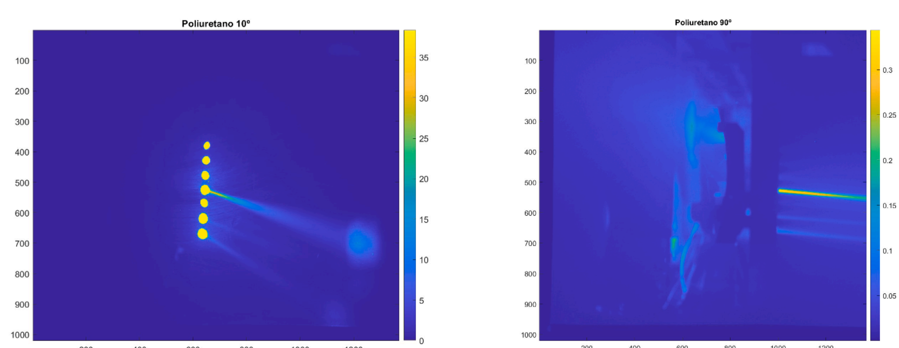

(a) (b)

Fig. 8. Representative measurements acquired using the Lumicam 1300, illustrating the multispectral behavior of light propagation in polyurethane smoke. Part of the experimental setup is shown, consisting of a vertical box mounted on a goniometer and containing LEDs operating at different wavelengths. Figure (a) corresponds to a measurement acquired with the light sources positioned at an angle of 10° relative to the observer, whereas Figure (b) corresponds to a configuration with the light sources rotated to an angle of 80°.

nance perceived by an observer through a simplified first-order scattering model.

The simulation tool developed in Matlab reproduces light propagation in smoke-filled environments using a three-dimensional model discretized into small elemental smoke volumes, as shown in Fig. 10. Each volume stores experimentally determined optical properties of the medium, including the phase function and the extinction coefficient, allowing the amount of light scattered toward the observer to be

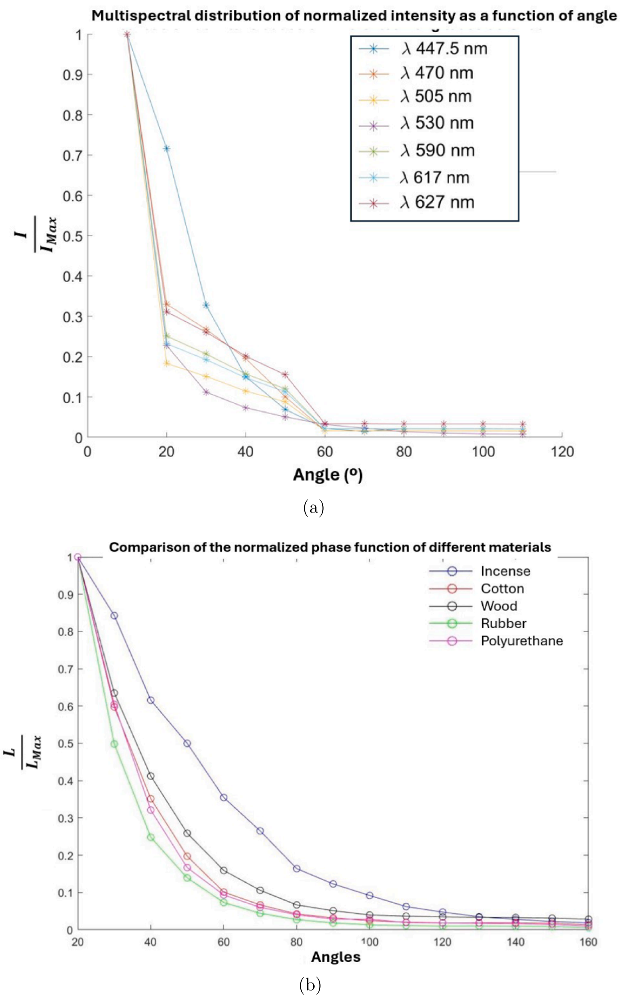

Fig. 9. (a) Normalized intensity distribution for polyurethane smoke. (b) Average normalized phase functions obtained for different materials, including incense, polyurethane, wood, and rubber.

calculated. The logical architecture of the software is organized into four main modules: definition of the simulation space, photometric characterization of the light source, definition of smoke optical properties, and calculation of perceived luminance, as illustrated in Fig. 11. The environment is represented by a three-dimensional matrix in which the relative positions of the light source, observer, and objects present in the scene are established.

Subsequently, the software processes .IES photometric files to reconstruct the angular luminous intensity distribution of the luminaires and interpolate it throughout the simulation space. The interaction between light and the scattering medium is then calculated using the experimentally obtained phase function for different smoke types together with the attenuation described by the Lambert–Beer law. For each elemental volume, the veiling luminance generated toward the observer is determined by considering both scattering and absorption along the optical path. Finally, the three-dimensional luminance distribution is projected

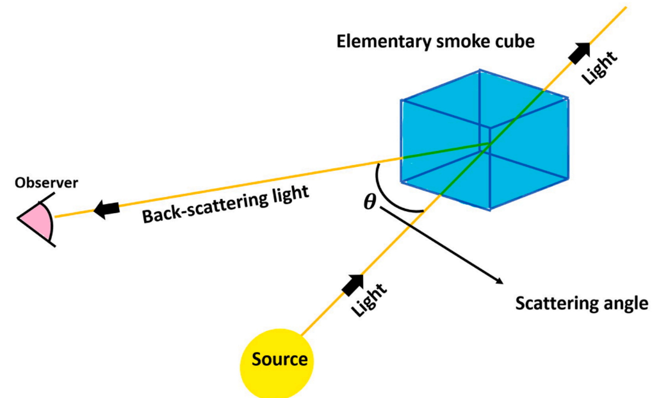

Fig. 10. Diagram illustrating the interaction of a volume element with incident light.

onto a two-dimensional plane, generating a perspective image that simulates the observer's visual perception in the presence of smoke, as shown in the schematic representation of Fig. 12.

The simulations shown in Fig. 13 correspond to a small-scale environment designed to reduce computational time. These simulations were performed using a luminaire emitting light exclusively toward a corridor located on the floor of the scene. The results illustrate how the luminance distribution perceived by an observer located near the ground varies depending on the amount of smoke present in the medium. The term "amount of smoke" refers to the optical smoke density within the environment, which can significantly affect both visibility and light scattering, as observed in the experimental stage.

Furthermore, Fig. 14 illustrates one of the capabilities of the software: the possibility of simulating different scene perspectives. This functionality allows multiple scene configurations to be developed in order to analyze light behavior under different conditions.

Finally, the software suggests that designing a luminaire to emit light preferentially toward a desired direction could increase the probability that an observer identifies safety elements within the environment. This behavior can be observed in Fig. 15, where the left image shows the entire scene illuminated, whereas in the right image only the corridor is illuminated. The simulations suggest favorable trends; however, objective validation using contrast metrics, luminance measurements, or observer-based experiments remains as future work.

6. Limitations of the experimental approach

The present work is limited to controlled experimental conditions and is not intended to reproduce the full complexity of a real fire scenario. The optical properties of smoke may vary significantly depending on the combustible material, combustion conditions, particle size distribution, and aerosol dynamics.

Furthermore, the implemented simulation model employs a simplified first-order scattering approximation and does not consider complex phenomena such as multiple scattering, turbulence, or dynamic smoke stratification. Therefore, the obtained results should be interpreted as relative trends observed under the considered experimental conditions.

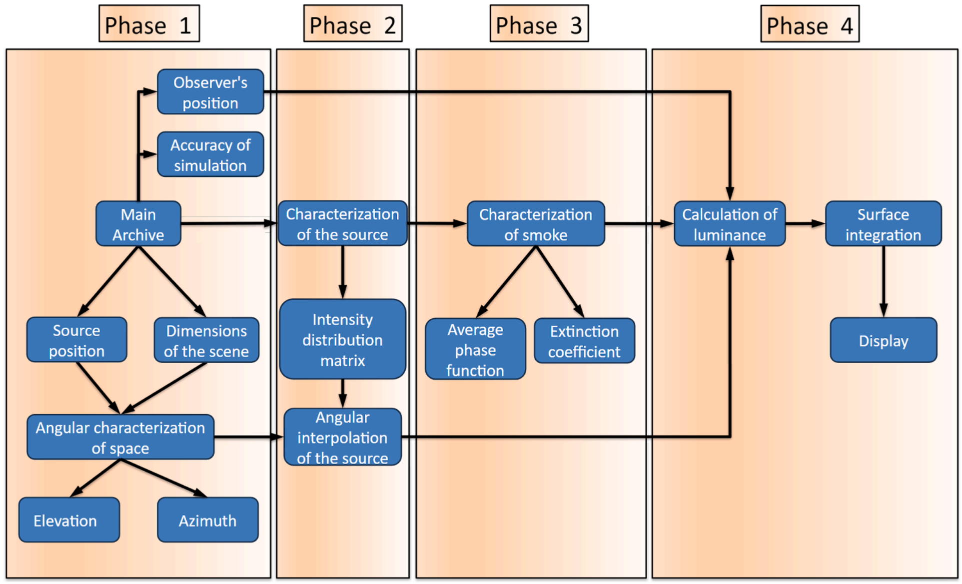

Fig. 11. Flow diagram of the developed simulation tool.

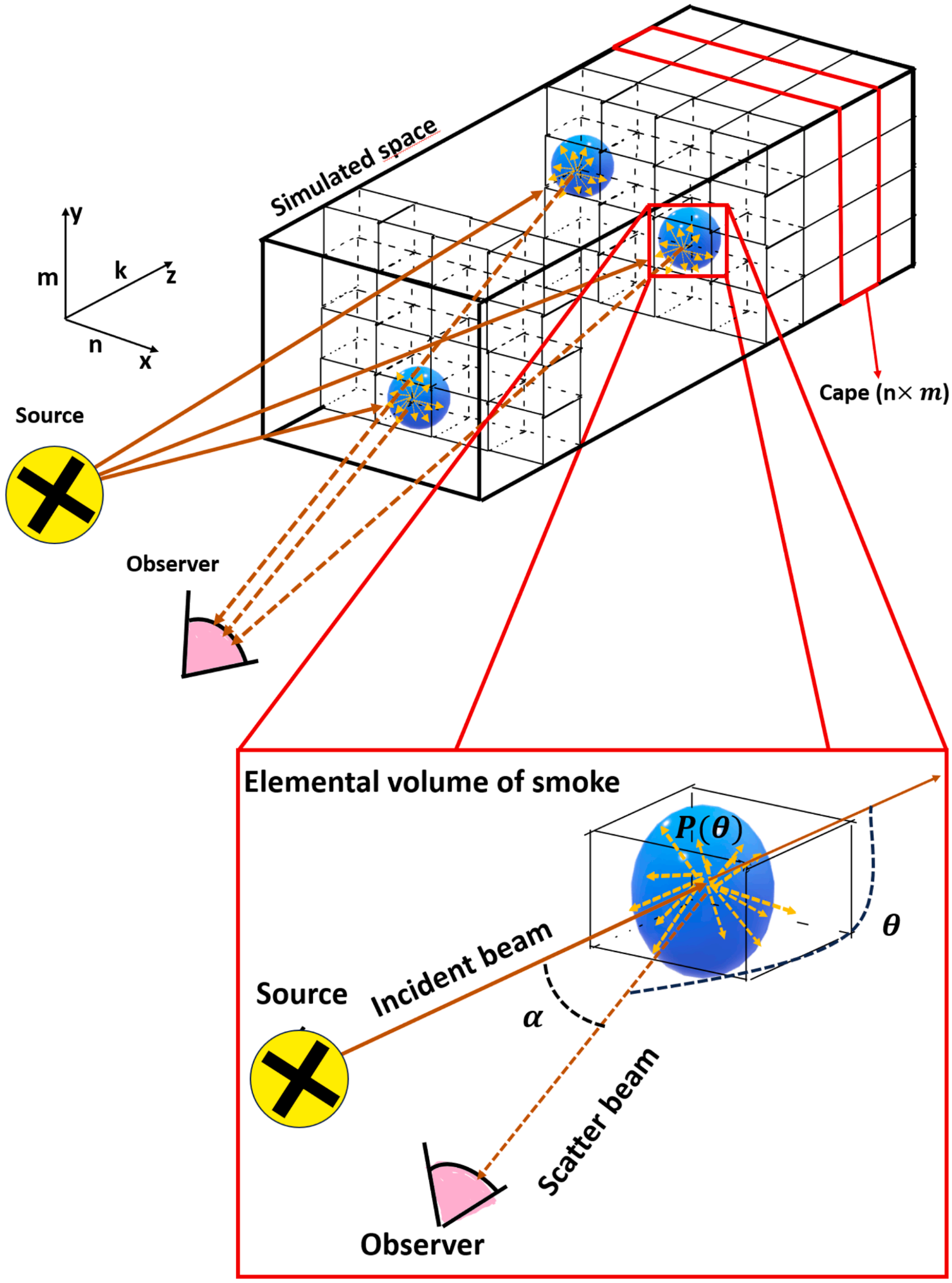

Fig. 12. General schematic representation of the simulation tool operation.

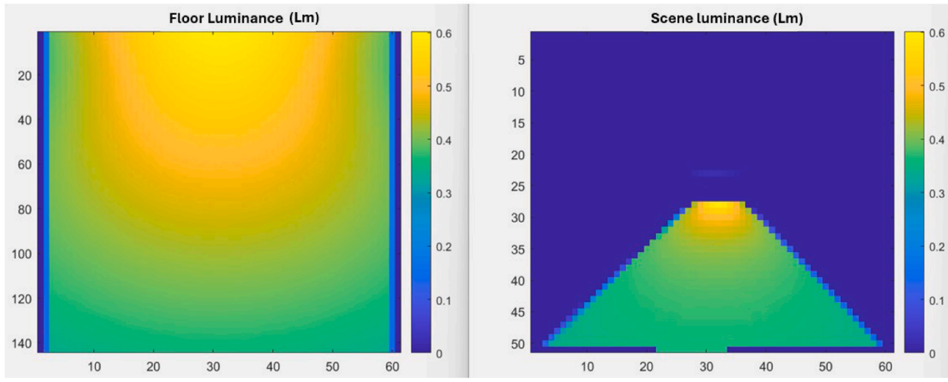

(a)

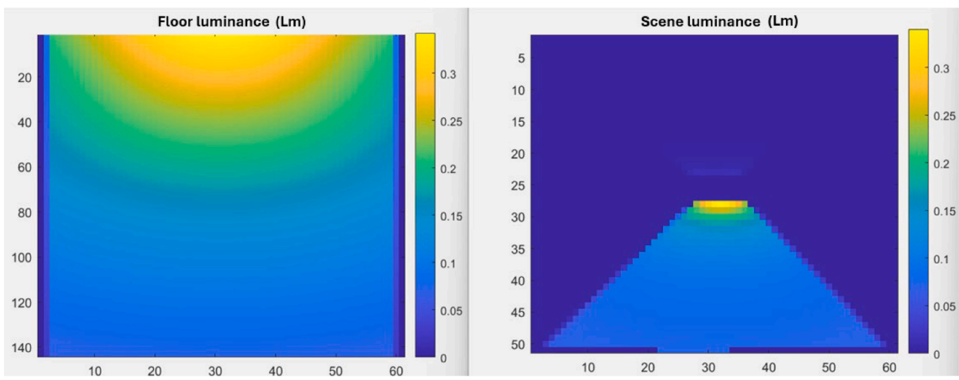

(b)

Fig. 13. Simulations of ground luminance distribution in the smoke chamber for different scenarios with an extinction coefficient of $0.2\ m^{-1}$. The simulations illustrate how the smoke distribution changes depending on the height occupied within the volume. In figure (a), the smoke layer is located 0.9 m above the ground, whereas in figure (b), the smoke layer is located 0.7 m above the ground. All simulations are shown from a lateral perspective corresponding to the observer viewpoint. The images on the left represent the luminaire intensity distribution mapped onto a matrix, while the images on the right show the resulting luminance distribution applied to a region of interest corresponding to a corridor.

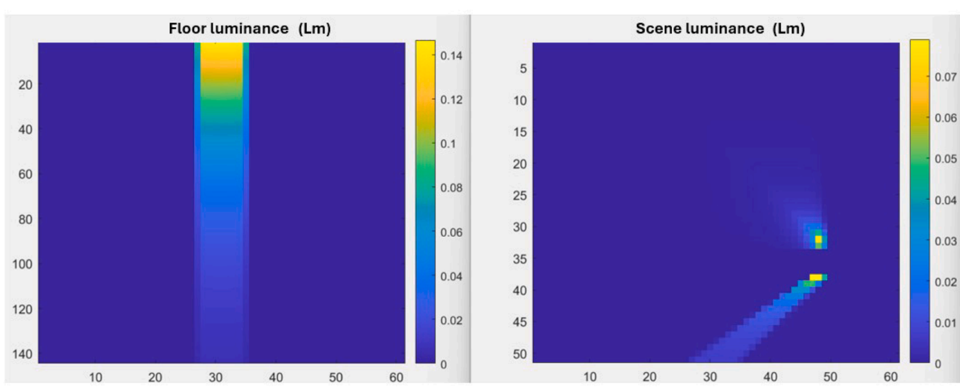

Fig. 14. Simulation of ground luminance distribution in the smoke chamber. The smoke layer is again located 0.9 m above the ground. The image on the left represents the luminaire intensity distribution mapped onto a matrix, while the image on the right shows the resulting luminance distribution applied to a corridor region of interest.

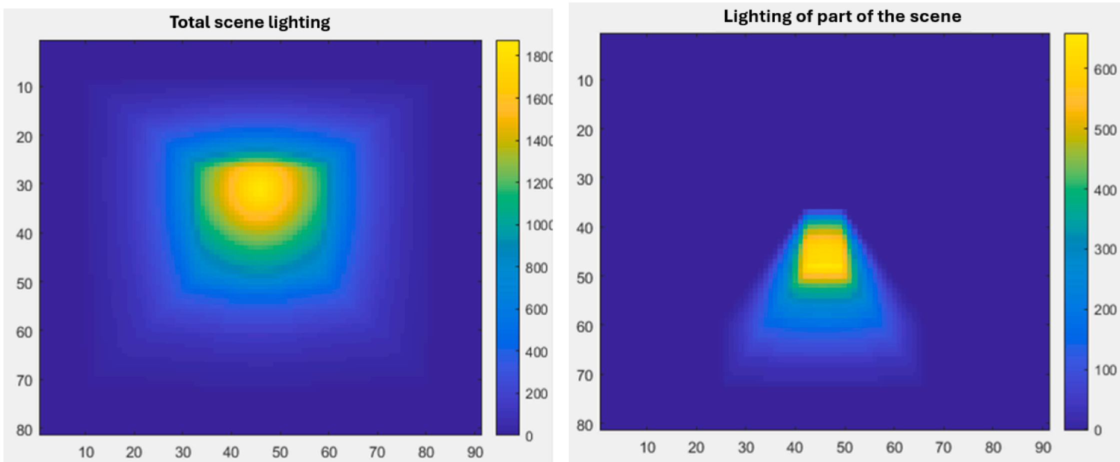

(a) (b)

Fig. 15. Simulation of a scene where, in the left image (a), a luminaire emitting in all spatial directions was used, whereas in the right image (b), the luminaire emits only toward the region of interest corresponding to a corridor.

7. Conclusions

This work presents an experimental methodology to study the interaction between light and smoke through the characterization of the spectral extinction coefficient and the angular distribution of light scattered by combustion-generated aerosols. To this end, two experimental configurations were developed under controlled laboratory conditions: 1 aimed at the spectral analysis of light attenuation and another focused on the angular study of the luminance perceived by an observer.

The performed experimental measurements show that smoke generated by different materials exhibits different optical behaviors in terms of both spectral extinction and angular redistribution of radiation. Under the tested conditions, certain spectral regions exhibit lower relative extinction levels than others, demonstrating the spectral dependence of light propagation in the presence of smoke.

Similarly, the performed angular measurements allow the analysis of light scattering trends associated with different geometric configurations between the light source, the aerosol, and the observer. Although the experimental procedure is not intended to fully reconstruct the theoretical phase function of the aerosol, the obtained results provide useful information regarding the angular distribution of luminance in smoke-filled environments.

The experimentally obtained optical parameters were subsequently incorporated into a simplified lighting simulation model intended for the analysis of spatial luminance distribution trends in environments with defined optical properties. The implemented simulation does not reproduce the complete dynamics of smoke propagation nor human visual behavior under real evacuation conditions, but rather constitutes an analysis tool based on experimentally measured optical parameters.

The obtained conclusions should be interpreted within the considered experimental conditions. The optical properties of smoke may vary significantly depending on the combustible material, combustion conditions, particle size distribution, and aerosol morphology. Therefore, future work should incorporate additional particle characterization techniques and more advanced scattering models in order to extend the scope of the presented results.

CRediT authorship contribution statement

J. Quintana Benito: Writing – original draft, Supervision, Software, Project administration, Investigation, Conceptualization; **B. Garcia-Fernandez:** Writing – review & editing, Conceptualization; **A. Álvarez Fernández-Balbuena:** Writing – review & editing, Conceptualization; **M. Duvisón Rodriguez:** Writing – review & editing, Investigation; **M. Jaureguizar Ortiz:** Writing – review & editing; **M. A. Garcia Perez:** Writing – review & editing, Conceptualization; **D. Váquez Molini:** Writing – review & editing, Supervision, Investigation, Formal analysis, Conceptualization.

Declaration of competing interest

The authors declare that they have no known competing financial interests or personal relationships that could have appeared to influence the work reported in this paper.

Data availability

Data will be made available on request.

References

[1] C. Rexfort, Combination of a fire model and a smoke sensor model, Fire Saf. J. 41 (4) (2006) 252–257.
[2] J.H. Klote, J.A. Milke, P.G. Turnbull, Handbook of Smoke Control Engineering, American Society of Heating, Refrigerating and Air-Conditioning Engineers, 2012. https://books.google.es/books?id=BZvfnQEACAAJ.
[3] K. Yonemitsu, A. Sasao, T. Oshima, S. Mimasaka, Y. Ohtsu, Y. Nishitani, Quantitative evaluation of volatile hydrocarbons in post-mortem blood in forensic autopsy cases of fire-related deaths, Forensic Sci. Int. 217 (1) (2012) 71–75. https://doi.org/10.1016/j.forsciint.2011.09.027
[4] B. Hahn, Research and conceptual design of sensor fusion for object detection in dense smoke environments, Appl. Sci. 12 (22) (2022) 11325.
[5] B. Karlsson, J.G. Quintiere, Enclosure Fire Dynamics, CRC Press, 1999.
[6] M.J. Hurley, D.T. Gottuk, R. Hall John, Jr., K. Harada, E.D. Kuligowski, M. Puchovsky, M. Watts John, Jr., C.J. Wieczorek, et al., SFPE Handbook Of Fire Protection Engineering, Springer, 2015.
[7] E. Ronchi, S.M.V. Gwynne, D.A. Purser, P. Colonna, Representation of the impact of smoke on agent walking speeds in evacuation models, Fire Technol. 49 (2) (2013) 411–431. https://doi.org/10.1007/s10694-012-0280-y
[8] M.S. Wright, G.K. Cook, G. Webber, The effects of smoke on people's walking speeds using overhead lighting and wayguidance provision, in: Proceedings of the 2nd International Symposium on Human Behaviour in Fire. MIT, Boston, 2001, pp. 275–284.
[9] K. Fujii, T. Sano, Y. Ohmiya, Influence of lit emergency signs and illuminated settings on walking speeds in smoky corridors, Fire Saf. J. 120 (2021) 103026. Fire Safety Science: Proceedings of the 13th International Symposium, https://doi.org/10.1016/j.firesaf.2020.103026
[10] J.S. Reid, T.F. Eck, S.A. Christopher, R. Koppmann, O. Dubovik, D.P. Eleuterio, B.N. Holben, E.A. Reid, J. Zhang, A review of biomass burning emissions Part III: intensive optical properties of biomass burning particles, Atmos. Chem. Phys. 5 (3) (2005) 827–849. https://doi.org/10.5194/acp-5-827-2005
[11] D.W. Weinert, T. Cleary, G. Mulholland, P.F. Beever, Light scattering characteristics and size distribution of smoke and nuisance aerosols, Fire Saf. Sci. 7 (2003) 209–220. https://doi.org/10.3801/IAFSS.FSS.7-209

[12] E. Perera, D. Litton, A detailed study of the properties of smoke particles produced from both flaming and non-flaming combustion of common mine combustibles, Fire Saf. Sci. 10 (2011) 213–226. https://doi.org/10.3801/IAFFS.FSS.10-213
[13] C. Gnendiger, T. Schultze, K. Börger, A. Belt, L. Arnold, Extinction coefficients from aerosol measurements, Fire Saf. J. 146 (2024) 104110. https://doi.org/10.1016/j.firesaf.2024.104110
[14] D. Burlacu, A.M. Georgescu, Ş.N. Trache, Small scale measurement of artificial smoke optical properties, in: IOP Conference Series: Earth and Environmental Science, 664, IOP Publishing, 2021, p. 012013.
[15] D. Burlacu, A.M. Georgescu, A.A. Vartires, I. Marinescu, An experimental evaluation of visibility in simulated smoke, in: 2019 International Conference on ENERGY and Environment (CIEM), IEEE, 2019, pp. 39–43.
[16] P. Coppa, A. La Malfa, Light extinction by fire smokes, J. Fire Sci. 15 (3) (1997) 180–202. https://doi.org/10.1177/073490419701500302
[17] J. Widmann, J. Duchez, J. Yang, J. Conny, G. Mulholland, Measurement of the Optical Extinction Coefficient of Combustion-Generated Aerosol Technical Note, Technical Report 36, National Institute of Standards and Technology, 2005. https://tsapps.nist.gov/publication/get_pdf.cfm?pub_id=101135.
[18] K. Kang, H. Macdonald, Modeling smoke visibility in CFD, Fire Saf. Sci. 8 (2005) 1265–1276. https://doi.org/10.3801/IAFSS.FSS.8-1265
[19] J. Tissot, M. Talbaut, J. Yon, A. Coppalle, A. Bescond, Spectral study of the smoke optical density in non-flaming condition, Procedia Eng. 62 (2013) 821–828. 9th Asia-oceania symposium on fire science and technology, https://doi.org/10.1016/j.proeng.2013.08.131
[20] T. Yamada, K. Kubota, N. Abe, A. Iida, Visibility of emergency exit signs and emergency lights through smoke, Fire Sci. Technol. 6 (2004) 560–568.
[21] L.T. Wong, K.C. Lo, Experimental study on visibility of exit signs in buildings, Build. Environ. 42 (4) (2007) 1836–1842. https://doi.org/10.1016/j.buildenv.2006.02.011
[22] J. Goo, Development of the size distribution of smoke particles in a compartment fire, Fire Saf. J. 47 (2012) 46–53.
[23] W.H. Dalzell, A.F. Sarofim, Optical constants of soot and their application to heat-flux calculations, J. Heat Transf. 91 (1) (1969) 100–104. https://doi.org/10.1115/1.3580063
[24] S. Li, X. Cheng, P. Mei, S. Lu, H. Yang, H. Zhang, Multiple scattering of light transmission in a smoke layer, Optik 125 (9) (2014) 2185–2190.
[25] M.E. Meyer, Particle Morphology And Elemental Composition Of Smoke Generated By Overheating Common Spacecraft Materials, Technical Report, 2015.
[26] M.R. Querry, Optical constants of minerals and other materials from the millimeter to the ultraviolet, 1987. https://api.semanticscholar.org/CorpusID:92855735.
[27] G.L. Wampfler, Light Transmitting and Light Scattering Properties of Smoke, 137, US Forest Products Laboratory, 1966.
[28] W. Wegrzynski, G. Vigne, Experimental and numerical evaluation of the influence of the soot yield on the visibility in smoke in CFD analysis, Fire Saf. J. 91 (2017) 389–398. Fire safety science: proceedings of the 12th international symposium, https://doi.org/10.1016/j.firesaf.2017.03.053
[29] A. Bideau-Mehu, Y. Guern, R. Abjean, A. Johannin-Gilles, Interferometric determination of the refractive index of carbon dioxide in the ultraviolet region, Opt. Commun. 9 (4) (1973) 432–434. https://doi.org/10.1016/0030-4018(73)90289-7